Toroidal rotation bifurcation with density in Tore Supra ohmically heated plasmas

J. Bernardo[1], C. Fenzi[2], C. Bourdelle[2], T. Aniel[2], J.- F. Artaud[2], J. Gunn[2], F. Clairet[2], P. Lotte[2], S. Cortes[3], J. P. S. Bizarro[1] and the Tore Supra team

[1] *Associação Euratom/IST, Instituto de Plasmas e Fusão Nuclear, Instituto Superior Técnico, Universidade Técnica de Lisboa, 1049-001 Libsoa, Portugal*

[2] *CEA, IRFM, F-13108 St Paul-lez-Durance, France*

[3] *Associação Euratom/IST, Instituto de Plasmas e Fusão Nuclear, Universidade da Beira Interior, 6201-001 Covilhã, Portugal*

1. Introduction

Understanding the underlying mechanisms of the so-called "intrinsic" plasma rotation (i.e. with no external momentum input) is of crucial importance for ITER, since the external torque delivered by the Neutral beam Injection systems is not foreseen to determine the overall velocity. Intrinsic plasma rotation can be understood as resulting from the competition of various mechanisms, as turbulence, MHD, fast particles and 3D (ripple, RMPs, …) driven effects.

Tore Supra (TS) is a large size tokamak ($R_0 \sim 2.4$m, a ~ 0.7m) with negligible external momentum input (P_{DNBI} ~350kW) and a strong magnetic field ripple, up to 7% at the plasma boundary. In this paper, the effect of density on intrinsic plasma rotation is examined in a set of Ohmic L-mode limited discharges, where ripple-induced neoclassical friction and turbulence driven mechanisms are therefore expected to be the main rotation driven mechanisms.

2. Plasma parameters and experimental conditions

The pulses used in this paper are a set of seven TS limited ohmic plasmas, where the plasma current I_p was 1 MA, the toroidal magnetic field was 3.6T, and the line integrated electron density n_l, was varied from $n_l \sim 2.25$ to 4.9×10^{19} m^{-2}. Plasma toroidal rotation is provided by Charge eXchange Recombination Spectroscopy (CXRS) diagnostic using the CVI ($\lambda = 5290.5$Å, n = 8→7) spectral line analysis. The Tore Supra CXRS system has 15 tangential viewing lines with spatial resolution ranging from 2 to 6 cm [1] (from the plasma edge to the core). In this experiment the time resolution was set to 15-20ms. The diagnostic uses a dedicated Neutral Beam Injection system (Deuterium beam), with nearly perpendicular injection, an injected energy of 55 keV and power of 350 kW. Since the momentum carried by the injected neutrals is rather low and can be negected, the system provides measurements for spontaneous toroidal rotation.

3. Experimental results

The plasma toroidal rotation (always counter-current here, corresponding to negative values) behaviour with density is illustrated in Figure 1, at three different normalized radii positions ($\varrho \sim 0.2, 0.6$ and 0.83) which are representative of three distinct plasma regions (core region $\rho < 0.5$, intermediate region $\rho = 0.5 - 0.7$, edge regions $\rho > 0.7$) where the rotation

behaviour is found to be different. In the core region (ρ = 0.2, Figure 1a), the rotation velocity is changed twice above certain density thresholds, first decreasing with density until $n_l \sim 3\times10^{19}$ m^{-2}, then increasing until $n_l \sim 3.5\times10^{19}$ m^{-2}, and decreasing again above. It is worth noting here that although this behaviour occurs inside and in the vicinity of the sawteeth inversion radius (r/a ~0.25), a possible link with the sawteeth behaviour can be discarded as the sawtooth period increases linearly (from 20 to 30ms) and no dramatic change was observed during the density ramp-up.

There are no similar behaviours observed in the intermediate (Figure 1b) or edge (Figure 1c) regions, where the velocity is found to decrease as the density increases, with a weaker dependency at the edge.

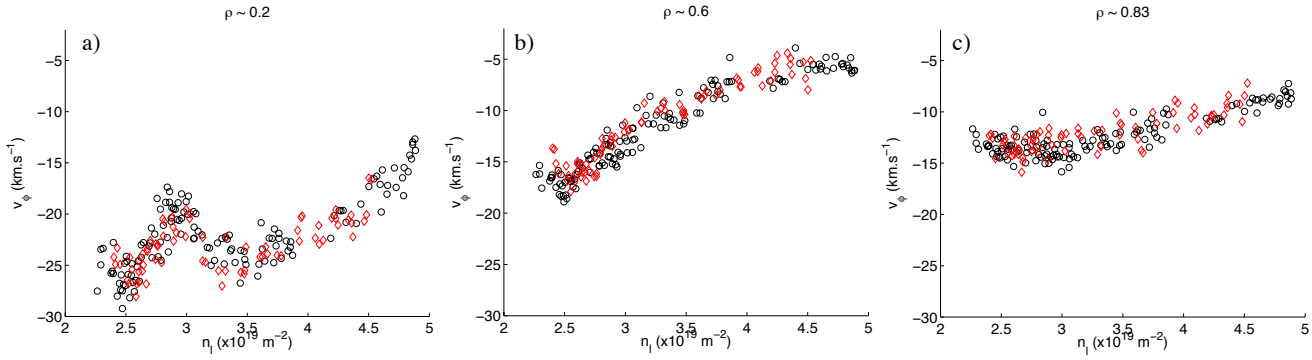

Fig.1– Toroidal velocity at $\varrho \sim 0.2, 0.6$ and 0.83 as a function of line integrated density for a set of 7 discharges. Red diamond symbols correspond to data from a single discharge.

Those observations can be compared to neoclassical predictions including the ripple-induced toroidal friction [2]. According to neoclassical predictions, the toroidal velocity can be written as $V_\phi = k_T \nabla T_i / eZ_i B_\theta$, with k_T = [1.67–3.54] depending on the ripple amplitude and the plasma collisionality. The neoclassical predictions for the toroidal velocity ("ripple-plateau" regime, $k_T = 1.67$) are reported as a function of the line integrated density in Figure 2 for a single discharge covering the whole density ramp-up (see red diamond data Figure 1, for ρ ~ 0.2, 0.6 and 0.8).

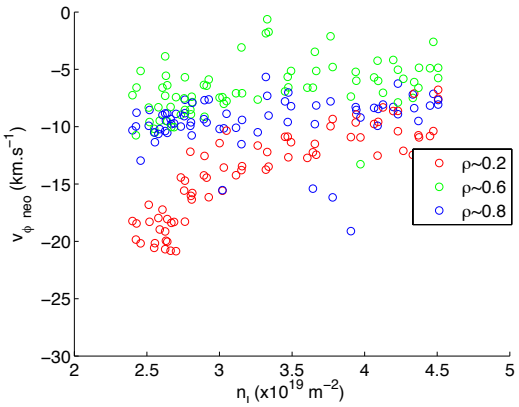

Fig.2– Toroidal velocity from ripple-plateau neoclasical predictions at $\varrho \sim 0.2, 0.6$ and 0.8 as a function of line integrated density.

It shows that predictions agree well with measurements (Figure 1) in terms of magnitude and sign, but the behaviours with density differ in the core (where no bifurcation is observed) and intermediate regions. The scatter observed for ϱ ~0.6 and 0.8 can be explained by the errorbars associated to ∇T_i, which is required for the neoclassical calculations. It is important to note that the toroidal rotation remains unchanged in the edge region (provided the measurement errorbars) during the density ramp-up. This observation is supported by reciprocating Mach probe measurements, showing no significant differences in the parallel Mach number at the begining (n_l ~2.76×10^{19} m^{-2}) and the end (4.25×10^{19} m^{-2}) of the density ramp (Figure 3).

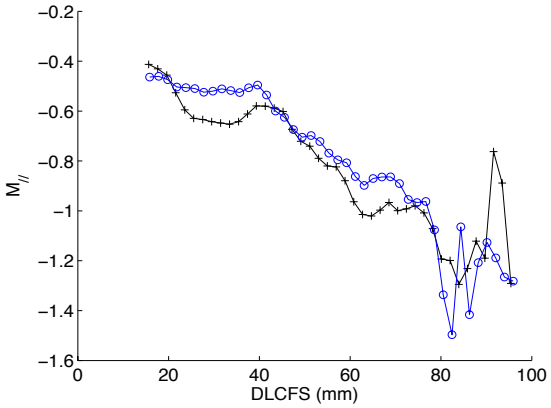

Fig.3- Parallel Mach number plotted as a function of the radial "distance from the LCFS" (DLCFS) at the beginning (black) and end (blue) of the density ramp.

In order to have a better understanding of the core toroidal rotation behaviour, turbulent mode analysis was performed using quasi-linear gyrokinetic simulations with the QuaLiKiz code [3]. Based on experimental profiles normalized at r/a=0.3 (Figure 4), QuaLiKiz simulations were performed using experimental profiles for the density while the ion and electron temperature were kept homothetic between themselves during the discharge in agreement with the experimental observations, see Figure 4.

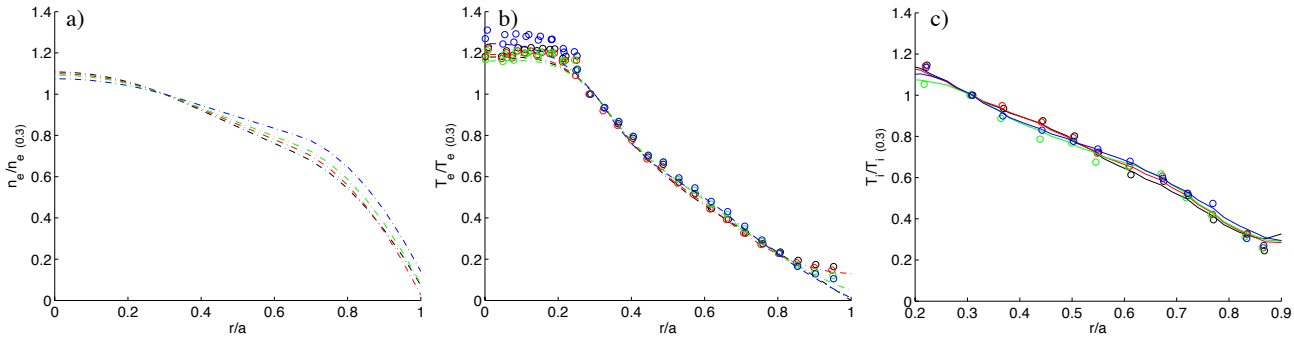

Fig.4– Normalized profiles at r/a=0.3 of a) electron density b) electron and c) ion temperature for 4 time slices during the density ramp.

As illustrated in Figure 5a, the plasma is found to be dominated by intermediate-scale

turbulence with peak growth rate at $k_\theta \varrho_s \sim 1$, indicating that trapped electron are contributing to the instabilities, which are nonetheless drifting in the ion drift direction. As the density is increased, the contribution of the high k modes is completely stabilized (Figure 5b) around $n_l \sim 3\times10^{19}$ m^{-2}, while lower k Ion Temperature Gradient (ITG) instability remains. The transition from ITG/TEM to pure ITG dominant instability as the density increases, and therefore collisionality, may provide an explanation for the first bifurcation occuring at $n_l \sim 3\times10^{19}$ m^{-2} (Figure 1a).

For the second rotation bifurcation occuring at $n_l \sim 3.5\times10^{19}$ m^{-2}, one possible mechanism could be linked to an increase in $\nabla v_{//}$, as it can be drawn from the analysis of Figures 1a and 1b. In contrast to TCV [4] and C-mod [5] observations, the observed rotation is always in the counter-current rotation, likely dominated by the ripple-induced toroidal friction [6]. The latter competes with turbulent momentum which could play an important role on these observations. Indeed, shear flow is well known to contribute to the residual stress [7] and therefore to the turbulent Reynolds stress. As reported in [8] both **E×B** and profile shearing mechanisms could be at play. Those points will be further investigated and adressed in a future work.

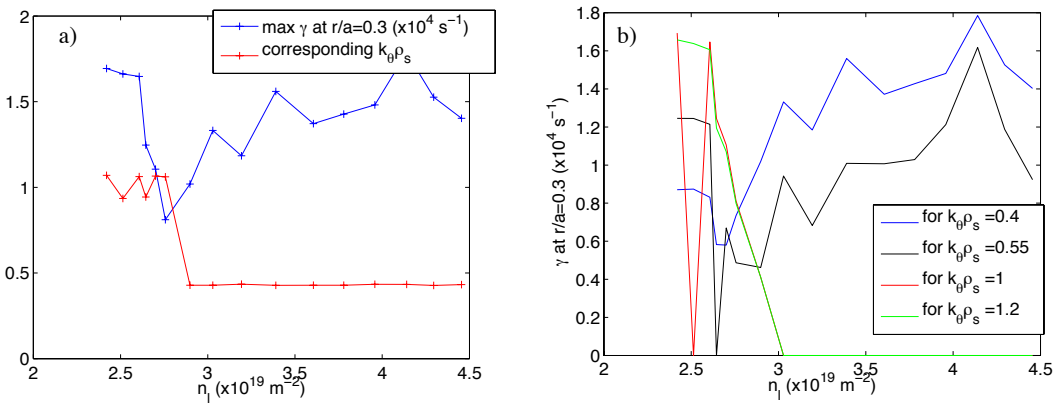

Fig.5– a) the maximum growth rate (blue) and respective $k_\theta \varrho_s$ (red), and b) growth rate for ITG/TEM normalized wavenumber range ($0.4<k_\theta \varrho_s<1.2$), at r/a=0.3 as a function of line integrated density.

Acknowledgments

This work, supported by the European Communities and 'Instituto Superior Técnico' under the Contract of Association between EURATOM and IST and EURATOM and CEA, has been carried out within the framework of the European Fusion Development Agreement. Financial support was also received from 'Fundação para a Ciência e Tecnologia' in the frame of the Contract of Associated Laboratory. The views and opinions expressed herein do not necessarily reflect those of the European Commission.

References

[1] C. Gil *et al* 2009 *Fusion Sci. Technol.* **56** 1219
[2] X. Garbet *et al.*, *Phys. Plasmas*, **17** (2010) 072505;
[3] C. Bourdelle *et al.*, *Phys. Plasmas*, **14** (2007) 112501.
[4] A. Bortolon *et al.*, Phys. Rev. Letter, **97** (2006) 235003;
[5] J. Rice *et al.*,Nuc. Fusion, **51** (2011) 083005;
[6] C. Fenzi *et al.*, *Nucl. Fusion*, **51** (2011) 103038;
[7] O.D. Gurcan *et al.*, *Phys.Plasmas,* **14** (2007) 042306;
[8] C. Angioni et al., *Phys. Rev. Letter*, **107** (2011), 215003.